Research Square

Preprints are preliminary reports that have not undergone peer review.
They should not be considered conclusive, used to inform clinical practice,
or referenced by the media as validated information.

Unraveling the hydraulic regulation mechanisms in iron-carbon materials enhanced anaerobic digestion of kitchen waste: Insights from carbon and nitrogen metabolismlllk

Qinyuan Shen
East China JiaoTong University
rui Gong
East China JiaoTong University
Yuying Hu
East China JiaoTong University
Bo Lei
17770826060@163.com

East China JiaoTong University
Daijin Wei
East China JiaoTong University
Mingming Tian
East China JiaoTong University

Research Article

Keywords:

Posted Date: November 12th, 2026

DOI: https://doi.org/10.21203/rs.3.rs-11298255/v1

License: This work is licensed under a Creative Commons Attribution 4.0 International License.
Read Full License

Unraveling the hydraulic regulation mechanisms in iron-carbon materials enhanced anaerobic digestion of kitchen waste: Insights from carbon and nitrogen metabolismlllk

Qingyuan-Shen[1,2],Rui Gong[1], Yuying Hu [1], Bo-Lei[1,*], Daijin Wei[1], Mingming Tian[1]

1. Jiangxi Provincial Key Laboratory of Environmental Pollution Control, Nanchang, Jiangxi, 330039,China
2. State Key Laboratory of Safety and Resilience of Civil Engineering in Mountain Area, Nanchang, Jiangxi, 330013,China

*. Correspondence:17770826060@163.com (B.L.)

This study investigated the effects of different rotation speeds on the performance, microbial communities, and carbon and nitrogen metabolism functions of an iron-carbon material-enhanced semi-continuous anaerobic digestion system for kitchen waste. The reactors were operated at 36 ± 1 ° C, an organic loading rate of 2.51 g VS/L/d, and a sludge retention time of 45 d, with four stirring conditions of 20, 60, 80, and 120 rpm. The results showed that the 60 rpm group achieved the highest average methane production rate of 492.0 mL/g VS, which was 5% – 7% higher than that of the other groups. Moderate stirring helped maintain stable concentration levels of volatile fatty acids and ammonia nitrogen. Community analysis showed that Chloroflexi, Bacteroidetes, Proteobacteria, and Firmicutes were the dominant bacterial phyla, while Methanothrix was the dominant methanogen. Functional analysis indicated that stirring at 60 rpm enhanced the potential for glycolysis, pyruvate metabolism, and volatile fatty acid metabolism, while promoting ammonia assimilation. Excessive stirring may enhance denitrification and intensify competition for carbon sources between denitrifying bacteria and methanogens.

1. Introduction

Kitchen waste is characterized by its large volume, high moisture content, abundance of organic matter, and susceptibility to decomposition. If not treated promptly and effectively, it can release foul odors, generate leachate and greenhouse gases, and promote the proliferation of pathogenic microorganisms, posing risks to the ecological environment and public health. At the same time, kitchen waste

contains large amounts of carbohydrates, proteins, and lipids (Chen et al., 2026a), giving it considerable potential for energy recovery and resource utilization.

Anaerobic digestion uses anaerobic microorganisms to convert complex organic matter into methane (Ajala et al., 2026) and carbon dioxide. Compared with treatment methods such as incineration, landfilling, and aerobic composting, anaerobic digestion offers the advantage of a high energy recovery rate and has been widely applied to organic waste treatment. However, kitchen waste has a complex composition and is prone to rapid acidification. Its anaerobic digestion process is susceptible to problems such as volatile fatty acid (VFA) accumulation, low methane production efficiency, and insufficient system stability (Chen et al., 2026b). In addition, the ammonia nitrogen produced during protein degradation may inhibit microorganisms under certain conditions, thereby affecting the long-term stable operation of the system.

Researchers have in recent years investigated the enhancement of addition such as biochar, activated carbon, magnetic materials, and iron-based conductive materials on high solid anaerobic digestion (HSAD). These materials provide attachment sites for microorganisms and may promote electron transfer between them. Chen et al. (Chen et al., 2026a) found that when the organic loading rate reached 8.0 g VS/L/d, methane production in the BC-Fe_2O_3 group increased to 625.66 mL/g VS, whereas that in the control group was only 261.01 mL/g VS. Under higher loading conditions (11.0 and 14.0 g VS/L/d), the BC-Fe_2O_3 group was still able to maintain methane production, while the control and BC groups failed to produce methane completely. In addition, oxygen-containing functional groups and iron of different valence states in the sludge-based iron-carbon composite mediator can promote electron transfer between microorganisms. This material can also enrich key functional microorganisms, thereby improving methane production rate (Wei et al., 2025).

In addition to additives, reactor mixing conditions are also an important factor affecting the efficiency of anaerobic digestion. For example, biogas recirculation can improve the vertical mixing and flow-field distribution of highly viscous substrates in the reactor. After mixing optimization, biogas production increased by 14.3%, while hydrogen sulfide emissions decreased by 59.4% (Shao et al., 2026). Wu et al. (Wu et al., 2026) reported that when the reactor height-to-diameter ratio was 2.4 and the mixing speed was 30 rpm, lipid conversion efficiency reached 96.3%. This indicates that appropriate hydrodynamic conditions can reduce lipid stratification and microbial inhibition, thereby improving anaerobic digestion performance. In anaerobic digestion systems enhanced with conductive materials, moderate mixing can promote mass

transfer and prevent the accumulation of organic acids. However, insufficient mixing may cause the conductive materials to settle and prevent adequate contact, whereas excessive mixing may disrupt microbial aggregates, impair methanogen activity, and increase energy consumption.

Currently, research on enhancing anaerobic digestion with iron-carbon materials has focused mainly on material type, dosage, and surface properties, while the synergistic effects between hydraulic conditions and iron-carbon materials have received insufficient attention. In addition, existing studies have mainly assessed enhancement effects using macroscopic indicators, such as methane production rate. However, the responses of carbon metabolism processes, including glycolysis, pyruvate metabolism, volatile fatty acid conversion, and the tricarboxylic acid cycle, remain poorly understood. The responses of nitrogen metabolism processes, such as denitrification, dissimilatory nitrate reduction, and ammonia assimilation, are also not well understood.

Accordingly, this study focuses on an iron-carbon material-enhanced anaerobic digestion system for kitchen waste and systematically investigates how different hydraulic conditions (rotation speeds: 20, 60, 80, and 120 rpm) regulate system performance and underlying metabolic mechanisms. The main research components include: (1) evaluating the system’s continuous operating performance at different rotation speeds and elucidating the patterns of methane production rate, VFA dynamics, and ammonia nitrogen variation; (2) analyzing the structural characteristics of bacterial and methanogenic communities; and (3) clarifying in depth the mechanisms by which hydraulic regulation affects key carbon metabolism processes and nitrogen metabolism processes. This study aims to provide a solid theoretical basis for optimizing process parameters and promoting the industrial application of iron-carbon enhanced anaerobic digestion technology.

2. Materials and Methods

2.1 Kitchen Waste and Inoculum

The substrate of kitchen waste (KW) was collected from the cafeteria of a university. KW was prepared according to the standard formulation previously established by our laboratory. It consisted of vegetables, meat, rice, and vegetable oil mixed in fixed proportions. The samples were processed using a grinder to reduce the

particle size to less than 1 mm and then stored at 4 ° C until use. The inoculum sludge was collected from a long-term, stably operated anaerobic digestion reactor. During the semicontinuous experiments, the total solids (TS) content of the kitchen waste was 32–38%, its volatile solids (VS) content was 30–34%, and its pH was 4–5; the TS content of the inoculum sludge was approximately 22%, its VS content was approximately 13%, and its pH was approximately 7.0.

2.2 Experimental Methods

The semicontinuous experiments were conducted in reactors with an effective volume of 1 L. The optimal parameters determined in the preliminary study were used: a total solids content of 12% and an iron-carbon microelectrolysis material dosage of 50 g/L. Under these conditions, the iron-carbon material was not prone to significant settling and could maintain sufficient contact with the microorganisms and substrate, thereby effectively enhancing anaerobic digestion. The SRT was set to 45 d, and the reactor temperature was maintained at 36 ± 1 °C using a circulating water bath. Four semicontinuous reactors were operated at rotation speeds of 20, 60, 80, and 120 rpm, respectively, with 2 min of mixing followed by a 2 min pause. They were designated R20, R60, R80, and R120, respectively. The experiment lasted 80 d in total, including a 30 d start-up period and a 50 d formal operation period.

2.3 Analytical Methods

The reactors were fed and discharged once daily at the same time. Biogas production and methane content were recorded, while pH and NH_3-N were measured every two days. Digestate was periodically withdrawn from each reactor and first centrifuged at 4000 rpm for 5 min to remove suspended particles. The supernatant was then passed through a membrane filter with a pore size of 0.45 μm, and the resulting filtrate was used to determine volatile fatty acids (VFAs). The biogas composition and concentrations of the various VFAs were analyzed using a gas chromatograph (GC6890, Shandong Tenghai Analytical Instruments Co., Ltd., China). To standardize the characterization of the concentrations of different VFAs, the measured results were converted to COD equivalents (mg COD/L). The conversion factors for acetic acid and propionic acid were 1.07 and 1.51 mg COD/mg, respectively; both n-butyric acid and isobutyric acid used a conversion factor of 1.82 mg COD/mg; and both n-valeric acid and isovaleric acid used a conversion factor of

2.04 mg COD/mg.

2.4 Metagenomic Analysis

Anaerobic digestate was collected for microbial analysis. Samples of anaerobic digestate from R20, R60 and R120 were stored frozen at −20 °C until analysis, after which metagenomic sequencing was commissioned. Samples from each reactor were collected at the end of the experiment and subjected to metagenomic sequencing analysis. Following genomic DNA extraction and quality assessment, the samples were used for sequencing library construction and Illumina high-throughput sequencing. The raw sequencing data were sequentially subjected to quality filtering and removal of contaminating sequences. Trimmomatic was used to remove adapter sequences and low-quality reads, while KneadData was further used to filter contaminating sequences, yielding high-quality valid sequences (clean reads). The valid sequences were then assembled using MEGAHIT, and assembly quality was assessed using QUAST. Taxonomic and functional annotation analyses were subsequently performed.

3. Results and Discussion

3.1 Effects of hydraulic regulation on the performance of iron–carbon material enhanced anaerobic digestion

The changes in methane production rate for each reactor during the semicontinuous anaerobic digestion of kitchen waste are shown in Fig 1(a). During the operation phase, the organic loading rate (OLR) was 2.51 g VS/(L • d), and the sludge retention time (SRT) was 45 d. In the first 30 days of operation, the methane production rate of each group fluctuated significantly; after day 30, the methane production rate gradually stabilized. During the stable operation phase, the average methane production rates of the R20, R60, R80, and R120 groups were 468.5, 492.0, 468.1, and 459.9 mL/g VS, respectively. Compared with the R20, R80, and R120 groups, the average methane production rate of the R60 group increased by 5.0%, 5.1%, and 7.0%, respectively. After day 30, the methane production rates of the R20, R60, R80, and R120 groups fluctuated within the ranges of 430 – 500, 440 – 520, 400 – 500, and 400 – 500 mL/g VS, respectively. Among them, the R60 group had the highest methane production rate, followed by the R20 group; when the rotation speed exceeded 60 rpm, the methane production rate decreased as the speed increased. This

indicates that 60 rpm may be beneficial to the mass transfer efficiency and microbial activity of the system, as it ensures sufficient mixing of the materials while avoiding the adverse effects of excessive shear force on the methanogenic community.

During the semi-continuous anaerobic digestion experiment, the changes in volatile fatty acids (VFAs) for each group are shown in Fig. 1(b). For the first 9 days, the total VFAs in each reactor were maintained between 350 mg COD/L and 550 mg COD/L, with acetic and propionic acids accounting for over 50% of the total VFAs across the four reactors. On day 11, the total VFA content in each reactor increased, reaching 573.6 mg COD/L, 572.2 mg COD/L, 563.5 mg COD/L, and 631.8 mg COD/L in the R20, R60, R80, and R120 groups, respectively. The pH values of all reactors also dropped to their lowest levels of the entire formal operation period. Throughout the experiment, the proportions of butyric and valeric acids in the R60 group remained relatively low without notable fluctuations. Studies indicate that the slow utilization of propionic and butyric acids easily leads to the accumulation of organic acids, which in turn causes acidification of the anaerobic digestion system and hinders methanogenesis (Liu et al., 2023).

The changes in ammonia nitrogen for each group are shown in the Fig. 1a. During anaerobic digestion, protein degradation leads to the accumulation of ammonia nitrogen in the system. Studies have shown that an ammonia nitrogen concentration below 3000 mg/L does not inhibit the anaerobic digestion of kitchen waste. Throughout the 50-day formal experiment, the ammonia nitrogen may not pose inhibition to the system. On day 11, the VFA content in each group increased, and correspondingly, the ammonia nitrogen content also rose. Subsequently, on day 13, the ammonia nitrogen content in R20, R60, R80 and R120 reached their peaks, after which the levels in all reactors began to decline, gradually stabilizing after day 21.

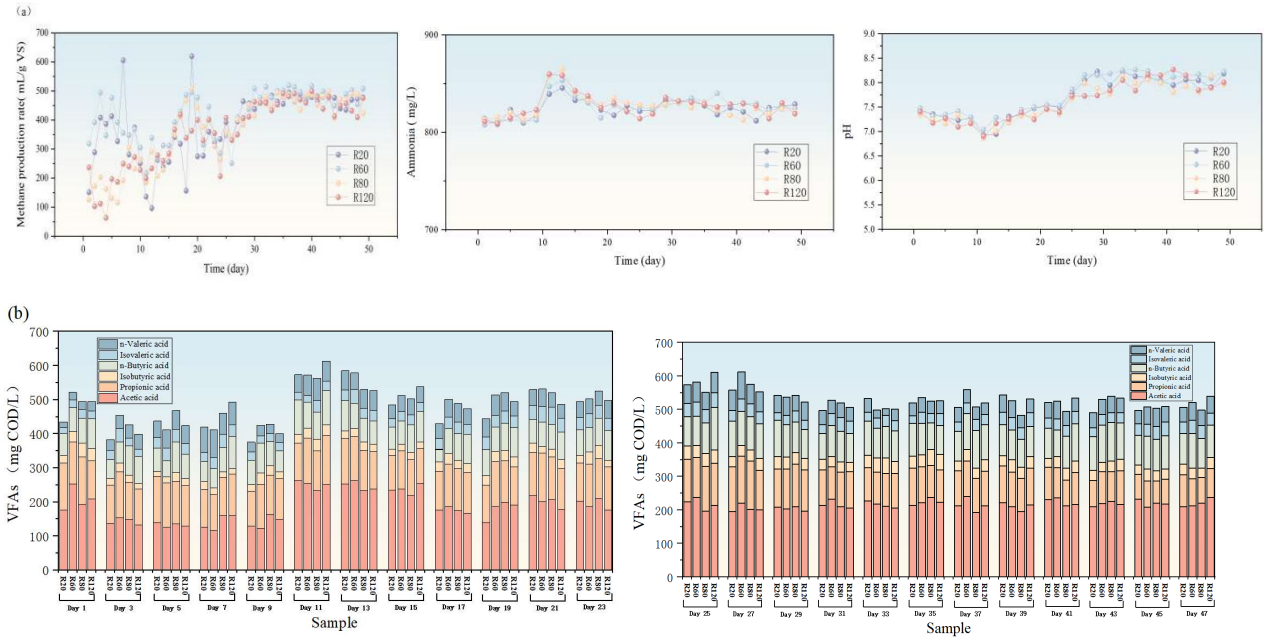


Fig. 1(a) Variations in methane production rate, ammonia nitrogen concentration, and pH during the operation period. (b) concentrations and compositional distributions of volatile fatty acids (VFAs) in each reactor on different sampling days.

3.2 Microbial community characteristics of iron–carbon material enhanced anaerobic digestion under hydraulic regulation

At the bacterial phylum level, the dominant bacteria in each reactor mainly included Chloroflexi, Bacteroidetes, Proteobacteria, and Firmicutes. Among them, Chloroflexi was the most abundant bacterial phylum. It has a strong capacity for organic matter degradation and can participate in carbohydrate hydrolysis and fermentation, as well as the conversion of volatile fatty acids (Zhang et al., 2026a). Bacteroidetes can secrete various hydrolytic enzymes that facilitate the breakdown of complex organic matter, such as polysaccharides and proteins, and produce intermediate metabolites such as acetate and propionate (Zhang et al., 2026a). Proteobacteria are involved in organic matter degradation, acid production, and nutrient transformation. Some members of Firmicutes can form endospores, making them highly tolerant of environmental changes, and contribute to the degradation of cellulose, proteins, and lipids (Yu et al., 2025; Zhang et al., 2026a). Additionally, Synergistetes can produce acetate, hydrogen, and carbon dioxide by fermenting amino acids and carbohydrates, and their growth is closely associated with the system's electroactive environment (Yu et al., 2025). Candidatus Cloacimonetes may be

involved in propionate oxidation and syntrophic metabolism (Alalawy et al., 2021). The above dominant bacteria jointly promote the hydrolysis, acidification, and acetogenesis of organic matter, continuously supplying substrates for methanogens and thereby sustaining methane production in the anaerobic digestion system.

At the family level, Kosmotogaceae, Synergistaceae, and Anaerolineaceae were the three most abundant families in the system. Kosmotogaceae may create favorable conditions for efficient methanogenesis by facilitating interspecies hydrogen transfer and acetate conversion while maintaining the system's redox balance (Gao et al., 2026). Synergistaceae are a typical group of syntrophic bacteria that can participate in direct interspecies electron transfer (DIET) (Zhang et al., 2026b). Additionally, the literature indicates that Synergistaceae can produce hydrogen through the metabolism of octadecane, while also generating substantial amounts of acetate (Eq. 9) (Qi et al., 2024). Anaerolineaceae is a functional bacterial family primarily involved in short-chain fatty acid (SCFA) oxidation. During anaerobic digestion, it provides methanogens with substrates by degrading short-chain fatty acids such as acetate and propionate, playing an important role in maintaining the system's methanogenic efficiency (Zhang et al., 2026b).

$$C_{18}H_{38} + 18H_2O \rightarrow 9CH_3COOH + 29H_2 \quad \Delta G^{o\prime} = -21\ kJ/mol \quad (9)$$

Methanothrix primarily produces methane via the acetoclastic pathway (Jiao et al., 2026). Methanolinea (Solon et al., 2026), Methanospirillum (Jiao et al., 2026), Methanoculleus and Methanobacterium (Seo et al., 2026) are hydrogenotrophic methanogens, which use hydrogen to reduce carbon dioxide and produce methane. Candidatus Methanofastidiosum primarily uses the methylotrophic methanogenesis pathway (Yang et al., 2025). Methanosarcina is a metabolically diverse group of methanogens that can use a variety of substrates, including acetate, hydrogen and carbon dioxide, and methylated compounds, to produce methane (Jiao et al., 2026). Considering the overall community composition, Methanothrix was dominant in the R20, R60, and R120 samples, indicating that methanogenesis in all three samples was predominantly driven by the acetoclastic pathway. The hydrogenotrophic pathway also played an important auxiliary role, whereas the contribution of the methylotrophic pathway was relatively minor.

3.3 Effects of hydraulic regulation on carbon metabolism in iron–carbon material enhanced anaerobic digestion

Core carbon metabolism primarily includes pathways such as glycolysis,

pyruvate metabolism, volatile fatty acid metabolism, and the tricarboxylic acid cycle (Cao et al., 2026). These pathways mediate the stepwise conversion of complex organic compounds such as starch and sucrose into pyruvate, acetyl-CoA, and volatile fatty acids, thereby providing substrates for subsequent methane production. Different stirring intensities may alter the abundance of relevant enzymes, affecting carbon source degradation and conversion, the production and consumption of volatile fatty acids, thereby influencing methane production in anaerobic digestion systems.

As a central pathway of energy and carbon metabolism, glycolysis catalyzes the conversion of monosaccharides to pyruvate, which is subsequently converted into volatile fatty acids (VFAs) through downstream fermentation pathways (Liu et al., 2026). In the R60 group, most enzymes involved in the initial stage of glycolysis were more abundant, indicating greater metabolic potential. Compared with R20, the abundance of EC 2.7.1.2 in R60 increased from $6.26 \times 10{-}4$ to $7.06 \times 10{-}4$, an increase of approximately 12.9%, which may facilitate the conversion of α-D-Glucose to α-D-Glucose-6P and thereby channel glucose into the central carbon metabolic network. EC 2.7.1.63 was also approximately 21.2% higher in R60 than in R20, indicating more active conversion between the relevant intermediates. Meanwhile, EC 3.1.3.10 increased by approximately 32.1%. These changes indicate that, compared with R20, R60 favors the entry of upstream carbon sources into downstream glycolysis, thereby providing substrates for pyruvate formation, VFA production, and methanogenesis.

β-D-Glucose can be converted to β-D-Glucose-6P and subsequently to D-Fructose-6P and D-Fructose-1,6P_2. Compared with R20, R60 showed increased relative abundances of most enzymes involved in this stage, suggesting that β-D-Glucose conversion and D-Fructose-1,6P_2 metabolism may be enhanced, thereby promoting Glyceraldehyde-3P formation.

Glyceraldehyde-3P is sequentially converted to Glycerate-1,3P_2, Glycerate-3P, and Glycerate-2P. Compared with R20, the relative abundances of EC 1.2.1.12 and EC 2.7.2.3 in R60 increased by 16.7% and 10.5%, respectively, indicating an enhanced potential for the conversion of Glyceraldehyde-3P to Glycerate-3P. EC 5.4.2.11 increased by 11.7% and 13.7% in R60 and R120, respectively, reaching its highest level in R120, which suggests that the interconversion between Glycerate-3P and Glycerate-2P may be promoted. In contrast, EC 5.4.2.12 decreased by 13.4% in R60 but partially recovered in R120, while EC 4.2.1.11 showed little variation among

the three groups. Overall, R60 promotes the sequential conversion of downstream glycolytic intermediates, whereas R120 retains a strong potential for glycerate metabolism.

In the terminal steps of glycolysis, EC 2.7.1.40, EC 2.7.9.1, and EC 2.7.9.2 were more abundant under R60 and R120 than under R20, suggesting that higher rotation speed may promote the conversion of phosphoenolpyruvate to pyruvate.

Pyruvate can be metabolized to acetate. Compared with R20, EC 2.3.1.8 and EC 2.7.2.1 increased by 4.1% and 2.1%, respectively, in R60, potentially further promoting the conversion of acetyl-CoA to acetate via acetyl-P. Although EC 2.3.1.12 and EC 6.2.1.13 were more abundant in R120, several key upstream ECs were less abundant than in R60. The metabolism in the anaerobic digestion system with the rotation speed of 60 rpm may provide substrates for acetoclastic methanogenesis and prevent excessive acetate accumulation by balancing substrate supply and consumption, thereby promoting methane production.

Propionate metabolism is a crucial link between organic acid conversion and methane production during anaerobic digestion. Compared with R20, R60 showed increases of 4.1% and 2.1% in EC 2.3.1.8 and EC 2.7.2.1, respectively, while EC 2.8.3.1 increased by 20.0%, indicating enhanced potential for the interconversion of propanoyl-CoA, propanoyl phosphate, and propanoate. It should be noted that the EC 2.3.1.8 and EC 2.7.2.1 also participate in the metabolism of pyruvate as mentioned before. Meanwhile, EC 5.4.99.2 increased by 3.3%, suggesting that the conversion of (R)-methylmalonyl-CoA to succinyl-CoA was enhanced. Notably, propionate can undergo syntrophic oxidation via the methylmalonyl-CoA pathway, and the timely consumption of acetate and hydrogen can reduce the thermodynamic barriers to this process; accordingly, the abundance of enzymes involved in these steps also increased (Zhang et al., 2025a). However, compared to R20, EC 2.1.3.1 and EC 2.8.3.27 decreased by 79.9% and 41.9%, respectively in R60, indicating that the pathway was not uniformly enhanced.

The butanoate metabolism analysis is as follows. Compared with R20, EC 2.7.2.7 and EC 2.3.1.19 increased by 24.1% and 23.2%, respectively, in R60. Metagenomic functional analysis indicated that the system's regulatory potential for the butanoate metabolic pathway was enhanced. Specifically, the abundances of genes associated with both the direct conversion of butanoate to butanoyl-CoA and the two-step cascade in which butanoate is first converted to the intermediate butanoyl-P

and then to butanoyl-CoA showed upward trends. Compared with R20, EC 1.3.8.1 increased by 17.2% in R60, potentially facilitating the conversion of butanoyl-CoA to crotonoyl-CoA. Downstream, EC 1.1.1.36 increased markedly by 428.6%, while EC 4.2.1.17 and EC 1.1.1.157 increased slightly. Meanwhile, EC 2.3.1.9 increased by 18.9%, indicating an overall enhancement in the functional potential for converting crotonoyl-CoA to acetoacetyl-CoA and acetyl-CoA. Except for EC 6.2.1.2, EC 4.2.1.55, EC 4.2.1.-, and EC 2.3.3.10, which decreased, all other enzymes were more abundant in R60 compared to those of R20. Under the R120 condition, the relative abundances of the relevant ECs were generally high, with most exceeding those in R20, suggesting that a higher stirring intensity is possibly more favorable for butanoate metabolism and promotes acetyl-CoA production.

TCA cycle-related functions differed under varied mixing conditions. The relative abundance of EC 1.1.1.42, which catalyzes the conversion of isocitrate to 2-oxoglutarate, increased from 5.51×10^{-5} in R20 to 6.03×10^{-5} in R120, whereas EC 1.1.1.37, which catalyzes the oxidation of (S)-malate to oxaloacetate, was most abundant in R20. Both EC 1.1.1.42 and EC 1.1.1.37 are key enzymes involved in NADH generation(Zhang et al., 2025a). This suggests that R120 may be more favorable for NADH generation at the isocitrate node, whereas R20 may primarily promote NADH generation during the conversion of (S)-malate to oxaloacetate. EC 6.2.1.5, which catalyzes the conversion of succinyl-CoA to succinate, reached its highest abundance of 4.03×10^{-4} in R60. This enzyme catalyzes the only reaction in the TCA cycle that directly generates ATP (Zhang et al., 2025a), indicating that R60 may have a relatively high ATP-generating potential. Overall, different mixing intensities may enhance distinct metabolic nodes within the TCA cycle: R20 possibly promotes (S)-malate oxidation and associated NADH generation, R60 possibly facilitates ATP generation at the succinyl-CoA stage, and R120 possibly enhances the NADH supply at the isocitrate stage. It was reported that ATP provides energy for carbon metabolism, while NADH serves as an electron donor whose electrons can be transferred along the respiratory chain to the conductive membrane (Zhang et al., 2025a). Thus, mixing intensity may alter the system’s energy-generation and electron-transfer potential by regulating key reactions in the TCA cycle, thereby affecting carbon metabolism.

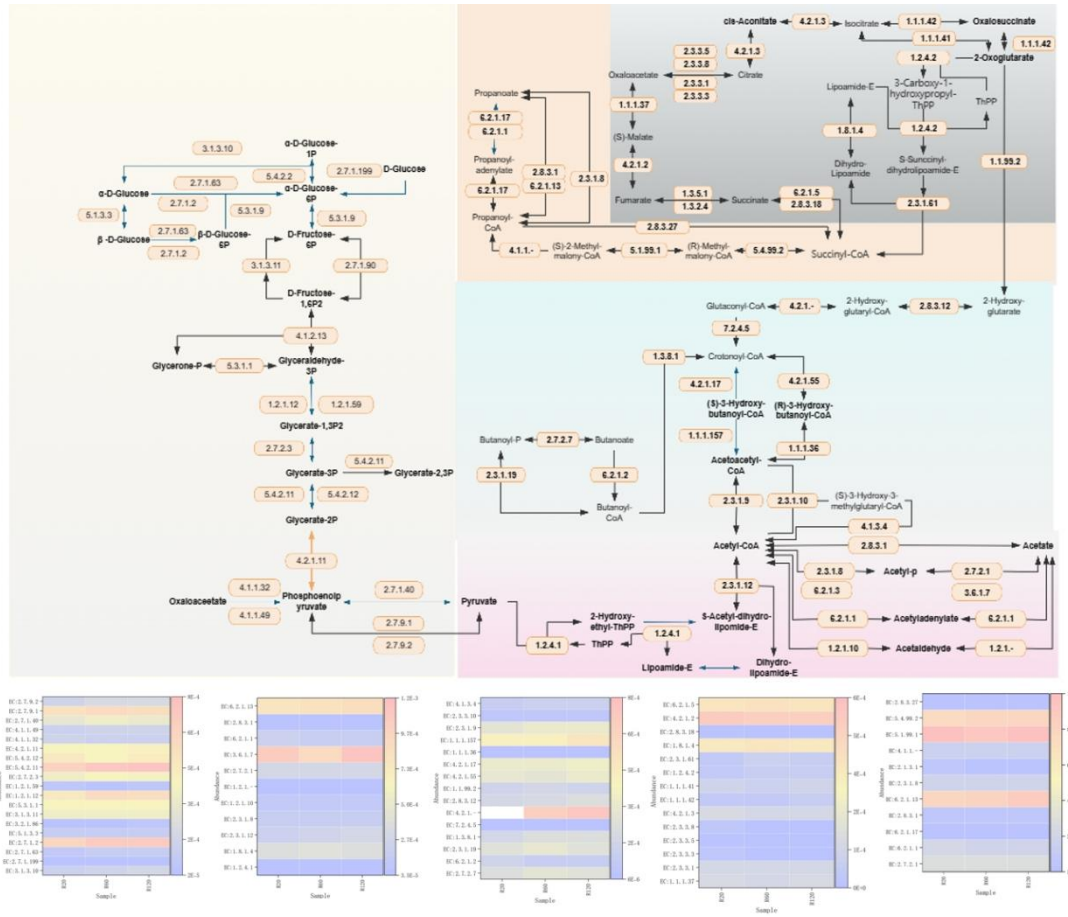


Fig.2 Carbon metabolic pathways and enzyme abundance in anaerobic digestion enhanced by iron–carbon materials

3.4 Effects of hydraulic regulation on nitrogen metabolism in iron–carbon material enhanced anaerobic digestion

While the biotransformation of nitrogenous substances sustains the nutritional needs of anaerobic digestion microorganisms, it also poses a risk of inducing system inhibition (Zhang et al., 2025b).

Denitrification is a biological process in which microorganisms gradually reduce nitrate or nitrite to nitrogen gas under anoxic conditions, serving as a crucial step in the nitrogen cycle. During the acetogenesis stage, denitrifying bacteria consume part of the carbon source for gas production, reducing the substrate available for methanogens (Qi et al., 2024). The denitrification pathway tended to be enhanced with increasing rotation speed. Compared to R20, the abundance of EC 1.7.5.1/1.7.99.-, which catalyzes the conversion of nitrate to nitrite, increased by 59.3% in R120; EC 1.7.2.1, which catalyzes the conversion of nitrite to nitric oxide, increased by 32.9%; and EC 1.7.2.5 and EC 1.7.2.4 increased by 24.5% and 52.7%,

respectively, possibly promoting the sequential conversion of nitrite oxide to nitrous oxide and nitrogen gas. The results indicate that increasing the rotation speed possibly enhance the complete denitrification potential from nitrate to nitrogen gas and reduce the accumulation of nitrogenous intermediates. Notably, the competition for carbon sources between methanogens and denitrifiers mainly occurs during the acetogenic stage of anaerobic digestion.

As mentioned above, with the increase in rotation speed, the abundance of EC 1.7.5.1/1.7.99.-, which catalyzes nitrate reduction, generally increases; meanwhile, the abundance of EC 1.7.2.2 and EC 1.7.1.15, which catalyze the reduction of nitrite to ammonium, shows little change. This suggests that high rotation speeds may promote the initial stage of the process, but have little impact on the potential for converting nitrite to ammonium.

Changes in the abundance of key enzyme genes during the assimilation of ammonia into L-glutamate are in response to rotation speed. The results showed that NAD-dependent glutamate dehydrogenase (EC 1.4.1.2) exhibited minor variations across different speeds, with fluctuations between the R20 and R120 groups remaining within 3%, suggesting that this enzyme is possibly insensitive to stirring intensity. In contrast, the abundance of NADP-dependent glutamate dehydrogenase (EC 1.4.1.4) was significantly upregulated (+10.8%) from R20 to R60, and then stabilized from R60 to R120. This indicates that increasing the stirring intensity to 60 rpm possibly activates this assimilation pathway, and further increasing the speed has a limited promotional effect on the relative abundance of enzyme. In summary, moderately enhancing stirring possibly improves mass transfer efficiency and increases the supply of intracellular reducing power (NADPH), thereby enhancing the microbial assimilation and utilization of free ammonia, which helps alleviate the potential inhibitory effects of high ammonia nitrogen environments on the system. The relevant reactions are shown in the equations (1) and (2).

$$\alpha\text{-Oxoglutarate} + NH_3 + NADH + H^+ \rightleftharpoons \text{L-glutamate} + NAD^+ + H_2O \quad (1)$$

$$\alpha\text{-Oxoglutarate} + NH_3 + NADPH + H^+ \rightleftharpoons \text{L-glutamate} + H_2O + NADP^+ \quad (2)$$

The GS–GOGAT pathway, which is jointly mediated by glutamine synthetase (GS, EC 6.3.1.2) and glutamate synthase (GOGAT, EC 1.4.1.13), is an important high-affinity ammonia assimilation pathway in microorganisms under low ammonia conditions. First, GS consumes ATP to incorporate ammonia into L-glutamate, producing L-glutamine. GOGAT then uses L-glutamine and α-ketoglutarate as

substrates to produce L-glutamate in the presence of reducing equivalents. The results showed that the abundance of GS-related enzymes varied little across rotation speed, with fluctuations of less than 3%, indicating that GS was possibly insensitive to changes in agitation intensity. In contrast, the abundance of GOGAT-related enzyme initially decreased and then recovered: compared with R20, it decreased by 8.4% at R60 and by 5.5% at R120. The relevant reactions are given in Eqs. (3) and (4).

$$ATP + L\text{-glutamate} + NH_3 \rightarrow ADP + phosphate + L\text{-glutamine} \quad (3)$$

$$L\text{-glutamine} + \alpha\text{-ketoglutarate} + NADPH + H^+ \rightarrow 2L\text{-glutamate} + NADP^+ \quad (4)$$

It can be inferred that as the rotation speed increases, microbial ammonia assimilation may partially shift from the GS-GOGAT pathway—which consumes more ATP but has a higher affinity for ammonia at low concentrations—to the less energy-intensive GDH-mediated direct reductive amination pathway. This shift may reflect adjustments in ammonia availability and cellular energy allocation strategies at different rotation speeds.

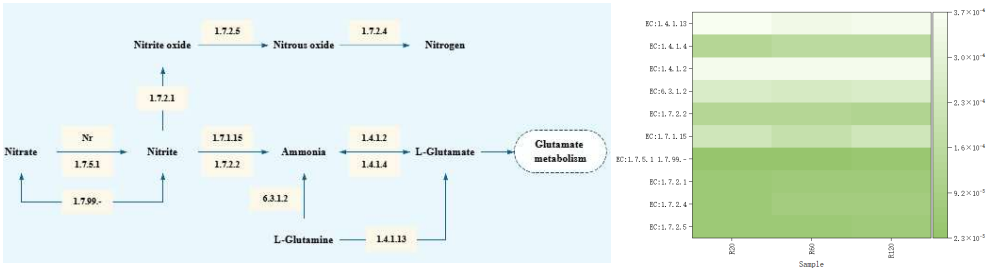


Fig.3 Nitrogen metabolism and the abundance of main related enzymes

3.5 Potential Mechanisms

Based on the overall system performance, microbial community structure, carbon and nitrogen metabolic functions, hydraulic regulation may enhance the effects of iron-carbon materials on anaerobic digestion by influencing microbial interactions, and metabolic flux distribution. The potential mechanisms are as follows:

(1) The R60 group exhibited an overall higher relative abundance of enzymes related to glycolysis, pyruvate metabolism, and VFA metabolism, which may promote the conversion of carbon sources into methanogenic substrates such as acetate, reduce the risk of organic acid accumulation, and continuously provide substrates for the dominant acetoclastic methanogen Methanothrix.

(2) Functional microbial groups such as Synergistaceae and Anaerolineaceae

may participate in interspecies electron transfer and short-chain fatty acid oxidation.

(3) Moderate mixing may promote ammonia assimilation via the GDH pathway, whereas excessively high rotation speeds may enhance denitrification potential, intensifying competition between denitrifying bacteria and methanogens for carbon sources during the acetogenesis stage.

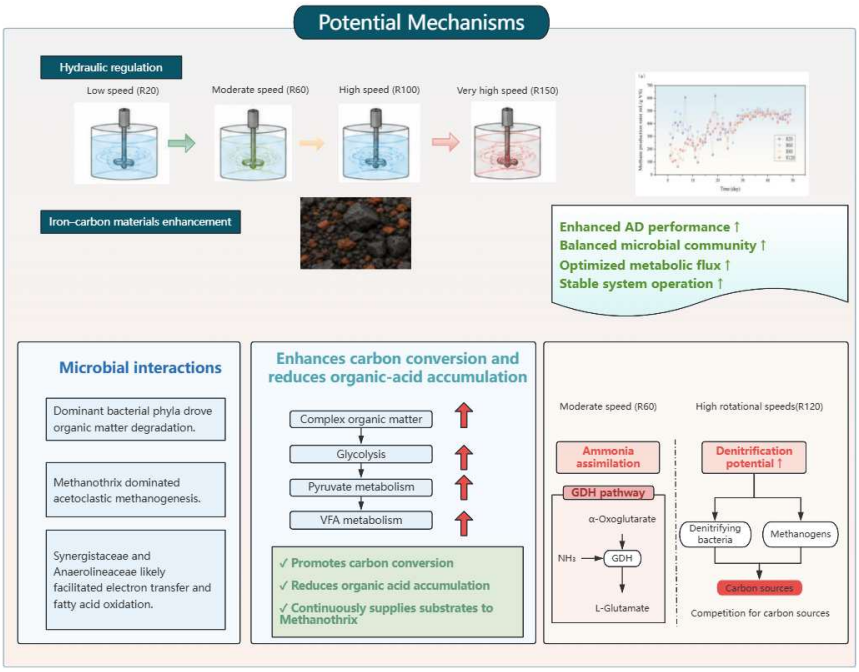


Fig.4 Mechanisms of hydraulic regulation and iron–carbon materials enhancing anaerobic digestion

4. Conclusion

This study investigated the effects of hydraulic regulation on the enhancement of anaerobic digestion of kitchen waste by iron-carbon materials. The results showed that moderate stirring increased methane production rate. At an organic loading rate of 2.51 g VS/(L • d) and a sludge retention time of 45 d, the R60 group achieved the highest average methane production rate, reaching 492.0 mL/g VS, which is 5.0%, 5.1%, and 7.0% higher than those of the R20, R80, and R120 groups, respectively. Microbial community analysis showed that the dominant bacterial phyla in the system included Chloroflexi, Bacteroidetes, Proteobacteria, and Firmicutes, while Methanothrix was the predominant methanogen, indicating that methane production mainly proceeded via the acetoclastic pathway. Metagenomic analysis showed that 60

rpm enhanced the metabolic potential for glycolysis, pyruvate metabolism, and volatile fatty acid metabolism, while promoting ammonia assimilation, thereby helping maintain the balance of carbon and nitrogen metabolism. Excessively high rotation speeds may intensify competition for carbon sources between denitrifying bacteria and methanogens.

Author Contributions

Qingyuan-Shen: Investigation, Data curation, Writing original draft. Rui Gong: Investigation Writing – Reviewing and Editing. Yuying Hu: Conceptualization, Writing – Reviewing and Editing. Bo-Lei: Writing – review and editing. Daijin Wei: Investigation. Mingming Tian: Investigation.

Funding

This work was supported by the Open Research Fund of Jiangxi Provincial Key Laboratory of Environmental Pollution Control (HJWRFZ-Z-2024-08).

Data Availability

The datasets generated during and/or analysed dur ing the current study are not publicly available but are available from the corresponding author on reasonable request

Declarations

Competing interests The authors have no competing interests to de clare that are relevant to the content of this article. Artificial intelligence assisted technology was only used during the writing process to improve the readability and language of the manuscript.

Reference

Ajala, O.O., Odejobi, O.J., Oke, E.O., Oyelade, J.O., Alao, A.I. and Adeoye, B.K. 2026. Modelling, optimization and computer-aided based techno-economic analysis of biogas production from anaerobic co-digestion of kitchen and animal wastes. Food and Bioproducts Processing 158, 332-347.

Alalawy, A.I., Guo, Z., Almutairi, F.M., El Rabey, H.A., Al-Duais, M.A., Mohammed, G.M., Almasoudi, F.M., Alotaibi, M.A., Salama, E.-S., Abomohra, A.E.-F. and Sakran, M.I. 2021. Explication of structural variations in the bacterial and archaeal community of anaerobic digestion sludges: An insight through metagenomics. Journal of Environmental Chemical Engineering 9(5), 105910.

Cao, S., Liu, X., Tao, Y., Ren, J., Zhou, Z. and Du, R. 2026. EPS-mediated mineralization drives granule densification and enhances denitratation–anammox coupling under alkaline conditions. Water Research 299, 125888.

Chen, G., Wang, Y., Mu, L., Cheng, Z., Li, Z., Dan, Z., Guo, H., Li, W. and Song, Y. 2026a. High-load semi-continuous anaerobic digestion of kitchen waste: Regulation by iron oxide-modified digestate-derived biochar and metagenomic analysis of microbial functions. Renewable Energy 264, 125576.

Chen, Y., Zhao, H., Liu, F., Zhang, X., Dai, X., Li, S. and Gu, L. 2026b. Elucidating the impacts of voltage application on construction of extracellular electron transfer in semi-continuous anaerobic digestion of kitchen waste. Renewable Energy 271, 125971.

Gao, Y., Liu, Z., Sun, Y., Wang, J., Wu, X., Lu, X. and Zhen, G. 2026. Mitigating perfluorooctanoic acid inhibition in electrochemically-assisted spiral upflow anaerobic membrane reactor for wastewater treatment: EPS interaction-desorption dynamics and metabolic pathway reconstruction. Water Research 289, 124761.

Jiao, D., Li, X., Liu, G., Feng, T. and Li, X. 2026. Thermal alkali pretreatment combined with magnetite to alleviate polystyrene microplastics inhibition and restrict TRGs propagation in anaerobic sludge digestion system. Journal of Water Process Engineering 87, 110099.

Liu, B., Pan, N., Sun, C., Xu, W., Song, W., Yan, L., Yan, T., Du, Y., Zhao, Y. and Gao, B. 2026. Distinct hydrolyzed Al-Ti species govern the coagulation behavior and subsequent anaerobic fermentation of CEPS sludge. Water Research 304, 126347.

Liu, Y., Wu, Z., Lv, Y., Jiang, L., Wei, Y., Li, Y.-Y. and Liu, J. 2023. Recovery of an acidified food waste anaerobic digestion reactor via NH4+-N and trace metals addition: Performance, microbial community response, and mechanisms. Journal of Cleaner Production 425, 138978.

Qi, M., Su, X., Zhao, W., Wang, Q. and Zhou, Y. 2024. Metabolic mechanisms of carbon and nitrogen interactions during anaerobic digestion of coal. Renewable Energy 237, 121653.

Seo, H., Lee, M.-E., Cho, S.-K., Im, S. and Ahn, Y. 2026. Intermittent low-strength ultrasonication enhances methane production by stimulating direct interspecies electron transfer in microbial electrolysis cell–anaerobic digestion systems. International Journal of Hydrogen Energy 251, 156159.

Shao, Z., Wang, W., Lai, R., Zhang, K., Li, J., Shi, G., Qiang, M., Song, J., Tan, H. and Chen, H. 2026. Optimized biogas recirculation hydrodynamics for process intensification in anaerobic digestion: Enhancing mixing while boosting methane production and H2S removal. Chemical Engineering Research and Design 230, 1104-1118.

Solon, T., Deaver, J.A. and Popat, S.C. 2026. Performance and microbial community dynamics in full-scale anaerobic co-digesters fed with fats, oils and grease. Bioresource Technology 458, 135068.

Wei, S., Guo, M., Guo, M., Li, M., Chen, W. and Jia, X. 2025. Sludge-based iron-carbon composite mediators enhanced simultaneous utilization of anaerobic sludge and biogas slurry in anaerobic digestion coupled with microbial electrolysis cell. Bioresource Technology 438, 133247.

Wu, L.-J., Duan, Y.-C., Hao, Z.-W., Xi, T., Yang, F. and Qin, Z.-F. 2026. Anaerobic digestion of oily food waste controlled by mixing intensity under high-lipid loading: Emphasis on the effect of height-to-diameter ratio on process performance, lipid conversion and microbial community. Process Safety and Environmental Protection 216, 109302.

Yang, Y., Huang, J., Qu, S., Wu, G., Liu, Y., Ling, Y., Sun, P., Zhao, Y. and Zhao, L. 2025. Detoxifying zinc oxide nanoparticles during sludge anaerobic digestion in the presence of polyferric sulfate. Journal of Environmental Chemical Engineering 13(5), 118652.

Yu, J., Usman, M., Liu, F., Schäfer, F., Shen, Y., Zheng, Z. and Cai, Y. 2025. CO2 agitation combined with magnetized biochar to alleviate “ammonia inhibited steady-state”: Exploring the mechanism by combining metagenomics with macroscopic indicators. Water Research 276, 123250.

Zhang, H.-C., Wan, L., Han, Y., Wang, X.C., Chen, R., Li, Y.-Y. and Xing, B.-S. 2026a. Unveiling dynamic membrane functions in a high-rate anaerobic mesophilic co-digestion system treating cow manure and food waste: Performance, digestate characteristics, and microbial community. Bioresource Technology 458, 135054.

Zhang, H., Zhang, S., Wei, P., Zhao, X., Chang, H., Mu, Z., Zhang, X., Liu, W., Liu, X., Su, X. and Wang, X. 2026b. Study on the mechanism of mixed biochar enhancing methane production in anaerobic digestion of corn straw. Biocatalysis and Agricultural Biotechnology 73, 104027.

Zhang, M., Han, Y., Zeng, Y., Wang, T., Wang, Z., Wu, Y., Li, N., Lobo, F.L. and Wang, X. 2025a. Understanding the microbial processes on carbon brushes that accelerate methanogenesis of long-chain fatty acids in anaerobic digestion. Water Research 273, 123084.

Zhang, P., Liu, X., Liu, Z. and Wu, D. 2025b. Iron-carbon composite promotes the conversion of nitrogen-containing substances during the anaerobic digestion of protein-rich substances. Bioresource Technology 436, 133057.